ACS APPLIED MATERIALS & INTERFACES

Research Article

www.acsami.org

Stability of Grafted Polymer Nanoscale Films toward Gamma Irradiation

Nikolay Borodinov,[†] James Giammarco,[†] Neil Patel,[‡] Anuradha Agarwal,[‡] Katie R. O'Donnell,[†] Courtney J. Kucera,[†] Luiz G. Jacobsohn,[†] and Igor Luzinov*[,†]

[†]Department of Materials Science and Engineering, and the Center for Optical Materials Science and Engineering Technologies (COMSET), Clemson University, Clemson, South Carolina 29634, United States

[‡]Microphotonics Center, Massachusetts Institute of Technology, Cambridge, Massachusetts 02139, United States

Supporting Information

ABSTRACT: The present article focuses on the influence of gamma irradiation on nanoscale polymer grafted films and explores avenues for improvements in their stability toward the ionizing radiation. In terms of applications, we concentrate on enrichment polymer layers (EPLs), which are polymer thin films employed in sensor devices for the detection of chemical and biological substances. Specifically, we have studied the influence of gamma irradiation on nanoscale poly(glycidyl methacrylate) (PGMA) grafted EPL films. First, it was determined that a significant level of cross-linking was caused by irradiation in pure PGMA films. The cross-linking is accompanied by the formation of conjugated ester, carbon double bonds, hydroxyl groups, ketone carbonyls, and the elimination of epoxy groups as determined by FTIR. Polystyrene, 4-amino-2,2,6,6-tetramethylpiperidine-1-oxyl, dimethylphenylsilanol, BaF_2, and gold nanoparticles were incorporated into the films and were found to mitigate different aspects of the radiation damage.

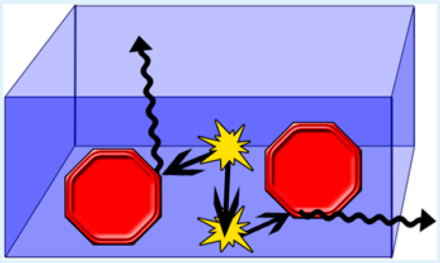

KEYWORDS: *grafted polymer films, gamma irradiation, radiation stability, enrichment polymer layers, nanoscale polymer films*

INTRODUCTION

Organic polymers possess unique functionalities and physical properties that can be utilized for a number of electronic and optical applications, ranging from memory devices to optical sensors.[1−9] As electronic/optical systems are scaled down to micron/submicron sizes, it has become critical to employ uniform, stable, and precisely located nanoscale polymer films in these devices.[3,4,8,10−14] To this end, chemically grafted polymer layers have recently been explored in the fabrication of components for a number of electronic and optical systems.[8,10,13−17] Covalent bonding to the substrate prevents the delocalization of the nanoscale polymer films, as a result of temperature/environmental variations and fluctuations. However, for a number of applications, functional polymer films must be designed to operate in drastically more challenging environments, such as high-energy γ radiation.

Ionizing radiation is well recognized for influencing mechanical properties, chemical composition, molecular weight, and the cross-linking extent of irradiated polymers.[18,19] The effects of irradiation on a number of polymers are known and understood. For instance, polymers such as polystyrene, aromatic polyamides, and polysulfones possess significant resistance to radiation damage, but others like polypropylene and poly(meth)acrylates will readily degrade upon exposure to ionizing radiation.[20−24] However, to the best of our knowledge, the radiation stability of ultrathin grafted polymer films has not been thoroughly investigated nor have effective mitigation strategies been outlined for these films. This is in spite of the fact that nanoscale polymer films have been considered to be employed in gamma irradiation dosimetry.[25−27] Therefore, in order to identify the application range for the systems containing grafted films, it is important to determine their radiation stability. In particular, this range is crucial for the devices being employed in orbiting satellites, spacecrafts, defense related applications, and the devices located in the vicinity of nuclear facilities or radioactive objects.[28,29]

In this regard, the present article focuses on the influence of gamma irradiation on submicron polymer grafted films and explores avenues for improving their stability toward radiation. In terms of applications, we concentrate on the polymer thin films employed in sensor devices for the detection of chemical and biological substances.[30−32] In fact, it is well established that enrichment polymer layers (EPLs) deposited on the surface of (optical) sensors can significantly improve their analytical performance, by attracting compounds of interest and increasing their local concentration in the vicinity of the sensing elements.[12,33−35] The effective and reliable functioning of an EPL is dependent on two main factors: the permanency of the chemical structure and the ability to absorb a significant amount of the chemical of interest through swelling. Both of these parameters can be significantly affected by an EPL's exposure to γ radiation, which is known to cause polymer cross-

Received: June 30, 2015
Accepted: August 10, 2015
Published: August 10, 2015

DOI: 10.1021/acsami.5b05863
ACS Appl. Mater. Interfaces 2015, 7, 19455−19465

linking (decreasing its ability to swell), as well as significant changes in the polymer chemical structure and molecular weight.

In our EPL designs, we use poly(glycidyl methacrylate) (PGMA), which was recently demonstrated to be an effective basic layer for the generation of a number of enrichment polymer layers.[10−12,36,37] This polymer belongs to the methacrylate polymer family, which is notoriously unstable when exposed to ionizing irradiation.[24] First, we follow the effects of gamma irradiation on the PGMA material and PGMA ultrathin films in terms of their chemical composition and swellability (cross-linking). Then, we demonstrate that the grafting of low molecular substances and polymers, as well as the incorporation of nanoparticles, significantly increases the stability of the nanoscale PGMA layer toward ionizing radiation.

EXPERIMENTAL SECTION

Materials. The PGMA was synthesized according to the previously published procedure.[38] The average molecular weight of the polymer used was 350−370 kDa, with a polydispersity index (PDI) of 2−3, measured in chloroform via gel-permeation chromatography (Waters Breeze), using polystyrene standards. Monocarboxy terminated polystyrene (PS), with an average molecular weight equal to 2.4 kDa and a PDI = 1.2 and the PS with an average molecular weight equal to 108.7 kDa and a PDI = 1.06 were both purchased from Polymer source, Inc. The dimethylphenylsilanol (DMPS) and 4-amino-2,2,6,6-tetramethylpiperidine-1-oxyl (4-amino-TEMPO) were purchased from Sigma-Aldrich. The Au nanoparticles (NPs) were purchased from *Nanoprobes*. They are stabilized with 1-mercapto-(triethylene glycol)methyl ether and have diameters of 5 ± 1 nm. The sulfuric acid and hydrogen peroxide were purchased from Sigma-Aldrich and LabChem Inc., respectively, and mixed at a 3:1 ratio to prepare the "piranha" solution. The synthesis of the BaF_2 NPs was conducted according to the procedures described elsewhere.[39,40] In brief, the synthesis was carried out via the solution precipitation method, using ammonium di-*N*-octadecyldithiophosphate (ADDP) as a ligand. A solution of the host and rare earth, RE, dopant metal nitrates dissolved in water was added to a solution of NH_4F dissolved in 1:1 ethanol:water, together with ADDP, to form nanoparticles in suspension. The barium fluoride nanoparticles have an average size of 30 nm [see the Supporting Information (SI) for more details]. The acetone, toluene, hexane, chloroform, and ethanol were purchased from Sigma-Aldrich, while the silicon wafers were obtained from WRS Materials.

Fabrication of Films. A dip-coating process from solution was employed to deposit a precursor polymer film on the silicon wafers using a dip-coater D-3400 (Mayer Feintechnik). Prior to the dip-coating, the silicon wafers were first cleaned in D.I. (deionized) water for 1 h using an ultrasonic bath, then placed in a piranha solution (3:1 concentrated sulfuric acid/30% hydrogen peroxide) at ∼80 °C and sonicated for 1 h, and finally rinsed several times with D.I. water. The polymer solutions for the coating were prepared with concentrations of 0.5%, 1%, 1.5%, and 2% w/v PGMA and 2% w/v PS. Chloroform was used as the solvent for all polymers. The polymer layers were deposited on the silicon surface by dip-coating at 320 mm/min. Thickness of nonmodified PGMA layers was 50 nm, the thickness of PGMA base layer for the preparation of modified nanoscale films was 25 nm (for subsequent PS grafting) and 70 nm (for 4-amino-TEMPO and DMPS grafting). The thickness of Au NPs/PGMA and BaF_2 NPs/PGMA layers was 90 and 140 nm, respectively.

In general, the PGMA layers were fabricated according to the previously published procedure.[41,42] The layers were annealed for 3 h at 130 °C in a vacuum oven, to anchor them to the silicon wafer. After annealing, the samples were rinsed 4 times with chloroform to remove any ungrafted polymer. For the PS grafting, we followed the procedure described in detail elsewhere.[42] In brief, the carboxy terminated PS (70%) was mixed in chloroform with high molecular weight PS (30%), to avoid dewetting during the polymer attachment. The mixture was dip-coated above the already grafted PGMA layer. Next, the PS was incorporated into the PGMA layer via melt grafting at 130 °C for 3 h. After annealing, the samples were rinsed 4 times with chloroform to remove any ungrafted polymer. To obtain the 4-amino-TEMPO/PGMA and DMPS/PGMA grafted layers, we followed the procedure described in detail elsewhere.[43] Briefly, 4-amino-TEMPO and DMPS were vapor-grafted into an already grated 70 nm PGMA layer at 130 °C for 1 h in a Schlenk tube. Next, the films were thoroughly washed with chloroform in order to remove any ungrafted substances. To obtain the nanoparticles/PGMA films, barium fluoride and gold particles were dispersed in a PGMA chloroform solution and dip-coated on the silicon wafer surface. The dry w/w contents of the barium fluoride and gold in the polymer films were 40% and 16%, respectively.

Characterization. Changes in the polymer layer thickness were registered with ellipsometry in order to estimate the extent of the grafting. The cross-linking extent of the nanoscale layers was estimated by solvent vapor swelling, and monitored by in situ ellipsometric measurements. For the swelling analysis, we used the procedure described in detail elsewhere.[11,12] It was conducted by placing the wafer covered with the films in a closed cell with a bucket of analyte. Ellipsometry was performed with a COMPEL automatic ellipsometer (InOmTech, Inc.), at an angle of incidence of 70°. The refractive index for the layers was assumed to be 1.5. Atomic force microscopy (AFM) studies were performed on a Dimension 3100 (Digital Instruments, Inc.) microscope. We used the tapping mode to image the surface morphology of the films, using silicon tips with spring constants of 50 N/m at scan rates in the range of 0.5 Hz.

Differential scanning calorimetry (DSC; model 2920; TA Instruments) was carried out at a heating rate of 20 °C/min. The FTIR spectra of the polymer nanoscale layers on 0.5 mm thick Si wafers were acquired using Thermo Nicolet 6700 FTIR spectrometry, equipped with the transmission accessory. A clean Si wafer from the same batch was used as a baseline for the transmission measurements, and 256 scans were averaged. For acquiring the ATR FTIR spectra of the bulk PGMA, the Thermo Nicolet Magna 550 FTIR spectrometer with the Thermo-Spectra Tech Endurance Foundation Series Diamond ATR accessory was used, and 16 scans were averaged. An ATR correction and baseline correction were performed using Thermo Scientific OMNIC software, versions 8.0 and 6.1. Deconvolution of the peaks and peak integration were completed using Origin MicroCal 6.1.

Irradiation. A Gammacell 220 gamma research irradiator, which produces γ rays with energies equal to 1.17 and 1.33 MeV during ^{60}Co decay, was used to irradiate the polymer samples studied here. The dose rate was 7 K rad/min calibrated with respect to the water. Absorption lengths for gamma irradiation in this range are much larger than the thicknesses of the samples tested. Therefore, the damage can be considered to be produced homogeneously throughout the material. Irradiation was performed at ambient temperature in air atmosphere. Bulk PGMA was subjected to dose of 1, 2, 5, 10, 15, and 30 Mrad. PGMA and (PS)/PGMA nanoscale films were subjected to dose of 1, 5, and 15 Mrad and (DMPS)/PGMA, (4-amino-TEMPO)/PGMA, Au NPs/PGMA, and BaF_2 NPs/PGMA were subjected to dose of 1 and 15 Mrad.

RESULTS AND DISCUSSION

PGMA Films. To obtain the EPL thin layer, the PGMA is initially deposited on the sensor elements by dip-coating, spin-coating, or drop-casting from solution and annealed at elevated temperatures.[10−12] In essence, the polymer films are anchored via the "grafting to" approach.[44] During annealing, in addition to a surface functional groups-epoxy reaction, a cross-linking reaction between the epoxy groups occurred. In essence, the PGMA layer is fabricated as a thin internally cross-linked film, covalently bound to the surface using its epoxy group functionalities.[38,44,45] The epoxy groups of the PGMA not involved in the reaction with the surface and cross-linking can

DOI: 10.1021/acsami.5b05863
ACS Appl. Mater. Interfaces 2015, 7, 19455−19465

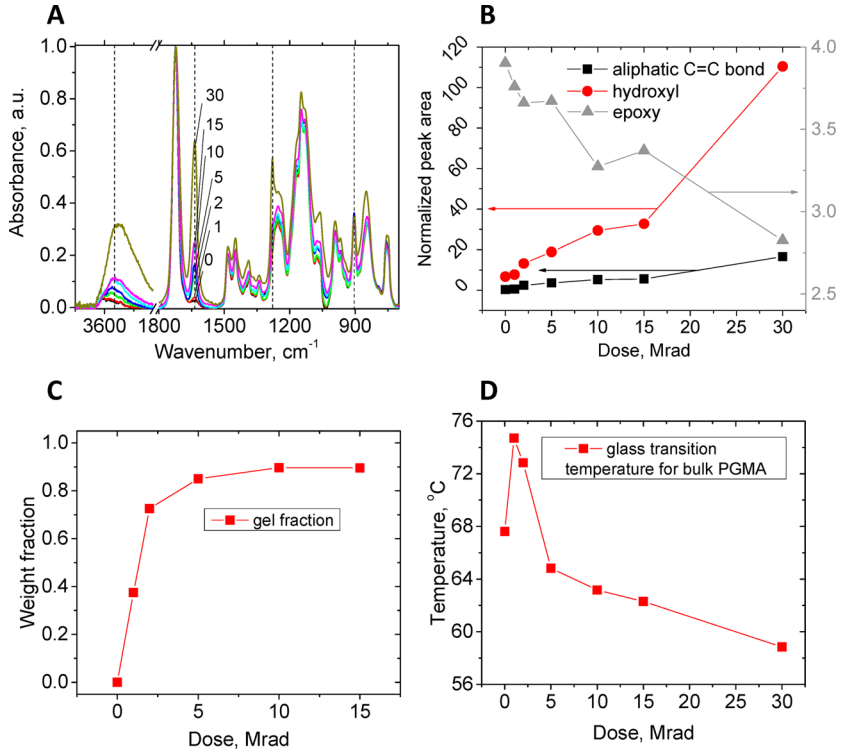

Figure 1. Gamma irradiation effects on bulk PGMA. (a) FTIR spectra of bulk PGMA samples before and after irradiation normalized by carbonyl peak, numbers on the graph correspond to the irradiation doses in Mrad; (b) areas of C═C peak, hydroxyl and epoxy peaks as a function of irradiation dose for bulk PGMA samples normalized by carbonyl peak; (c) gel-fraction of bulk PGMA samples versus dose of γ radiation; (d) glass transition temperature of bulk PGMA samples as a function of irradiation dose. Lines are guide for eyes only.

be used for the grafting of other polymer chains, to modify the chemical composition of the nanoscale film. In fact, the polymer was demonstrated to be an effective anchoring layer for grafting polymers to inorganic and polymeric surfaces, using the "grafting to" and "grafting from" approaches.[43,46−48]

Typically for polymers exposed to gamma irradiation (a) bond cleavage resulted in molecular weight decrease, (b) cross-linking of the polymer molecules led to network formation and an increase in molecular weight, (c) carbon dioxide was released because of carbonyl groups elimination, and (d) double bond formation that occurs as the result of radical recombination can be expected.[19] In this respect, the closest analogue to PGMA, the γ radiation stability of which has been rigorously studied, is poly(methyl methacrylate) (PMMA).[21,49−52] PMMA has been extensively used as an engineering plastic, organic glass, and a positive photoresist for electron beam lithography.[24] It is well documented that the radiation stability of PMMA is low in comparison with many other polymers.

Radiation Stability of Bulk PGMA. It is necessary to point out that, to the best of our knowledge, the data on the γ radiation stability of PGMA has not been reported in the scientific literature. Therefore, to understand the behavior of the PGMA nanoscale films upon their exposure to ionizing radiation, we first studied the influence of gamma irradiation on the PGMA bulk material. Figure 1a displays the ATR FTIR spectra of the bulk PGMA samples subjected to different doses of irradiation. First of all, we observe the appearance of the conjugated ester peak (1280 cm^{-1}), which is increasing with dose, during the PGMA material irradiation. In addition, the dose increase causes the intensive formation of carbon−carbon double bonds, which is indicated by the presence of an IR peak located at 1640 cm^{-1}. This process is well documented for PMMA degradation under irradiation.[24,53−55] The formation of conjugated esters occurs when a hydrogen atom is abstracted from the cut polymer main chain, and the resulting radical undergoes β-scission, resulting in the formation of a neighboring double bond and ester group.

With respect to the molecular weight, two main effects of ionizing irradiation on polymers have been identified: (a) chain scission decreasing molecular weight and (b) cross-linking increasing molecular weight.[56] Extensive cross-linking also leads to the formation of a nonsoluble fraction (gel-fraction) of polymer material. When the well-studied PMMA is exposed to gamma irradiation, it experiences an extensive main-chain scission/decrease in molecular weight. The polymer is not capable of cross-linking.[56−58] It is necessary to highlight a significant difference between the PGMA and PMMA macromolecules, which is the presence of reactive epoxy groups in the PGMA structure. We observed that under irradiation a certain amount of epoxy groups is consumed, as indicated by the decreasing of the 900 cm^{-1} band (Figure 1a,b). It is improbable that the epoxy groups are reacting with the radical species formed during the irradiation, since the PGMA is routinely obtained (including this work) by radical polymerization, which implies no interaction between the oxirane group and polymer chain carrying radical. Therefore, we suggest that the nucleophile-type initiation of the epoxy polymerization with alcohol and/or carboxyl groups[59] is responsible for the decrease in the epoxy group concentration. In fact, in the PGMA FTIR spectra, the presence of a small amount of hydroxyl groups was observed in the 3500 cm^{-1} spectral region (Figure 1a).

The presence of the hydroxyl signal in the spectra indicated that, prior to the irradiation, a small fraction of (a) epoxy

DOI: 10.1021/acsami.5b05863
ACS Appl. Mater. Interfaces 2015, 7, 19455−19465

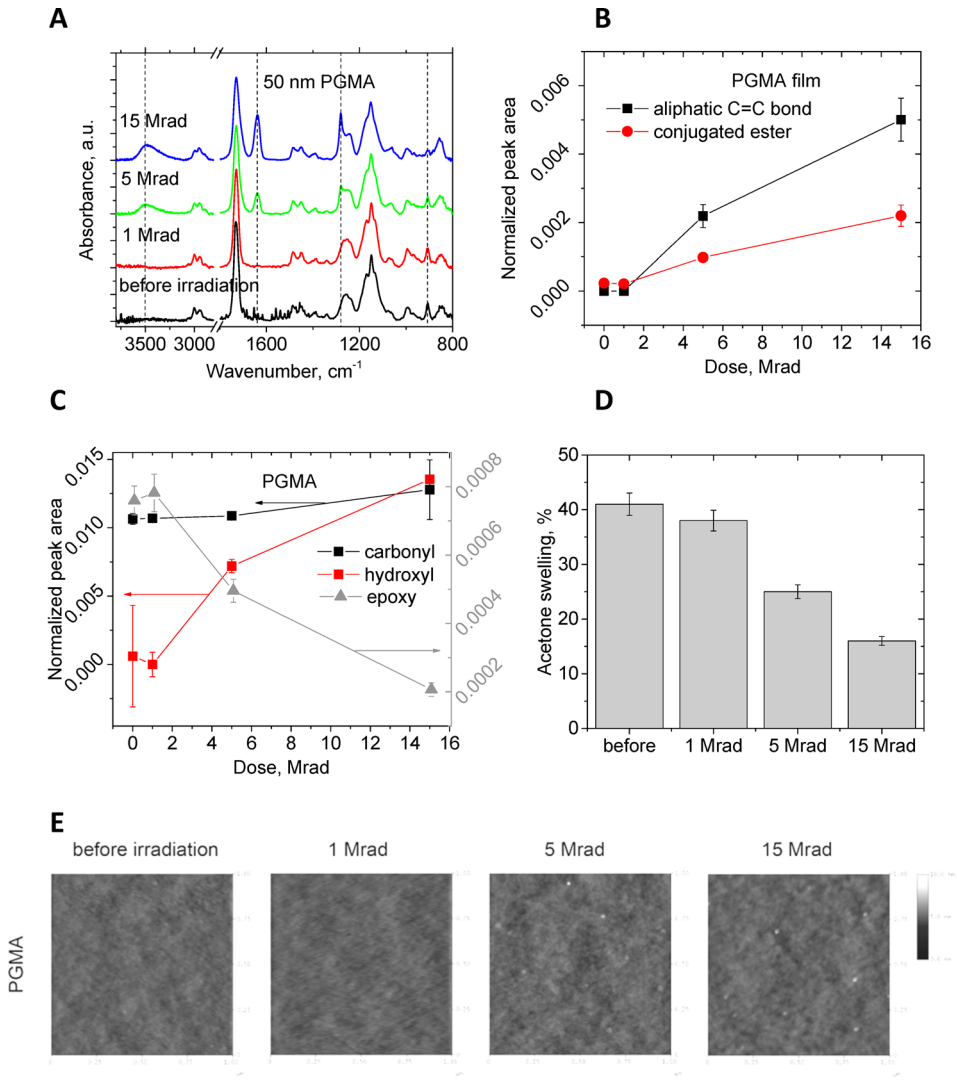

Figure 2. Gamma irradiation effects on PGMA grafted film. (a) FTIR spectra of PGMA film before irradiation, after 1, 5, and 15 Mrad gamma irradiation; (b) the areas of aliphatic carbon−carbon double bond and conjugated ester as a function of irradiation dose normalized by PGMA content; (c) the areas of carbonyl, hydroxyl (left axis), and epoxy (right axis) peaks normalized by PGMA content as a function of irradiation dose; (d) swelling extent in acetone vapor for PGMA films versus γ radiation dose; (e) AFM images (height bar is 10 nm, scan size 1 μm by 1 μm) of PGMA films. Lines are guide for eyes only.

groups in the macromolecules was opened, yielding hydroxyls, and/or (b) glycidyl methacrylate groups were hydrolyzed yielding carboxylic groups. During irradiation, the increased mobility of the (newly formed by chain scission) short chains facilitates the reaction between the hydroxyl and epoxy groups, since the shorter chains are less restricted from reptation movements than the original "frozen" below glass transition temperature (T_g) long chain.[60] The process is also driven by the increase in the concentration of the hydroxyl groups in the course of irradiation (Figure 1a). In the irradiated PMMA samples, a similar increase in the hydroxyl functionalities was observed and suggested to originate from the oxidative degradation of the polymer.[24]

In principle, our FTIR results indicate that under irradiation, PGMA simultaneously undergoes bond cleavage/chain scission and cross-linking via the epoxy groups. Both processes change the chemical nature of the polymer but influence its physical behavior in opposite directions: (a) cross-linking leads to an increase in the effective molecular weight, formation of the network, and decrease in the mobility of the macromolecule constituting material, while (b) bond cleavage/chain scission leads to a decrease in the effective molecular weight and an increase in the mobility of the macromolecule constituting material. It is necessary to point out that the level of cross-linking can be critical for the polymer layer employed as the EPL, since the extensive cross-linking decreases the ability of the enrichment layers to swell and attract the compounds of interest to the sensor elements.

In order to evaluate the level of the PGMA cross-linking, we determined the amount of the gel-fraction in the irradiated material as a function of the γ radiation dose. It was found that a dose increase up to 5 Mrad leads to an increase in the gel-fraction (Figure 1c). A further dose increase does not produce a significant change in the gel-fraction. Therefore, it appears that the cross-linking dominates the bond cleavage until reaching a dose of 5 Mrad. We have studied the thermal behavior of the irradiated polymer to reveal additional details of the degradation processes. Figure 1d shows the results of the DSC measurements of the PGMA glass transition temperature, which mostly reflects changes in the level of cross-linking and

DOI: 10.1021/acsami.5b05863
ACS Appl. Mater. Interfaces 2015, 7, 19455−19465

the molecular weight of the polymer chains. We found that the T_g rises from 68 to 75 °C at the initial (1 Mrad) stage of the radiation treatment. Further irradiation leads to a gradual T_g decrease, which reaches 59 °C after a dose of 30 Mrad. This result indicates that, initially, the formation of the polymer network hinders the mobility of polymer chains, and increases the thermal energy required to achieve long-range chain motions. However, when the dose reaches 5 Mrad, the chains in the network are cleaved to a certain extent, removing the excessive restrictions imposed on the chain movements by the cross-linking. The resulting effect is the growing number of shorter chains within the network with a lower T_g. These data shows the critical importance of monitoring the chemical composition of the nanoscale polymer layer, as well as its ability to swell when the radiation dose increases.

Radiation Stability of PGMA Nanoscale Films. We used ~50 nm PGMA layer, grafted to a silicon wafer, to study the influence of radiation on chemically grafted nanoscale films. First, we determined that within the range studied (dose up to 15 Mrad) the thickness of the film is unchanging. This result indicates that a measurable amount of the gaseous products is not formed during irradiation. In order to monitor the chemical changes of the irradiated PGMA nanoscale films, FTIR analysis before and after each step of the radiation treatment was performed for the grafted layers (Figure 2a–c). We found that the number of carbonyl groups in the films slightly increases under gamma irradiation (Figure 2a,c). It was documented that both the loss of carbonyls (primarily caused by −COOH group elimination) and formation of new ketone carbonyls can occur under irradiation.[49,53] The deconvolution of the carbonyl peak into ester (1730 cm^{-1}) and ketone (1710 cm^{-1}) peak components provided quantitative information about the gradual changes observed for the carbonyl peak, while the dose of gamma irradiation increases (SI, Figure S4, Table S1). The ester component area stays constant within the statistical errors, while the ketone component area develops for the irradiated PGMA nanoscale films.

As for the bulk PGMA, we observed the formation of a conjugated ester (peak at 1280 cm^{-1}) and double bond (peak at 1640 cm^{-1}) upon irradiation (Figure 2a,b). According to the infrared data, γ radiation also induces the formation of hydroxyl groups in PGMA, while the intensity of the oxirane (epoxy) ring vibration (ca. 900 cm^{-1}) gradually decreases (Figure 2c). This observation corresponds to the epoxy ring opening, accompanied by a hydroxyl peak appearing at ca. 3500 cm^{-1}. The area of the epoxy peak located at 900 cm^{-1} decreases 6 times for pure PGMA nanofilm after 15 Mrad, while the OH peak gradually increases with the increasing dose. This supports the mechanism of the epoxy rings opening being directly related to the hydroxyl-mediated reaction. In general, the FTIR results show that the radiation induced degradation of the PGMA grafted layer follows the same pathway as the degradation of the bulk polymer.

Additionally, we investigated how the extent of the PGMA film swelling in acetone vapor (the ratio between the thickness of the swollen film to its initial thickness) changes as a function of the radiation dose. The measurements allow the estimation of the level of the film cross-linking. Figure 2d shows that the swellability of the film in acetone gradually decreases with the dose. The results clearly indicate that gamma irradiation causes significant cross-linking of the 50 nm PGMA films.

It was reported that gamma irradiation can increase the surface roughness of the polymer materials.[61] Therefore, in order to investigate the surface morphology change in the irradiated PGMA nanofilms, the samples were imaged by AFM in the tapping mode (Figure 2e). The surface morphology of the irradiated polymer layers was found to be uniform and even, while the PGMA films remained smooth throughout the irradiation process, showing no discernible changes up to at least 15 Mrad. The AFM RMS (Root Mean Square) roughness for all layers was found to be 0.2–0.3 nm within 1 × 1 μm area (SI **Table S2**).

In general, we found that irradiation has a significant effect on the chemical composition and swelling extent of the nanoscale PGMA films. The changes definitely decrease the sensing ability of the PGMA based EPLs; therefore, strategies to increase the radiation stability of the PGMA based nanoscale films need to be identified.

Mitigation Strategies for Nanoscale PGMA Films. The general approach for the mitigation of the radiation effect on the PGMA nanoscale films is depicted in Figure 3. It is well-known that gamma irradiation initially causes the formation of radicals that are further involved in multiple reactions, including interactions with the oxygen present in the air, chain transfer reactions by hydrogen abstraction, and termination by recombination or disproportionation.[24] These processes cause critical morphological, topological, and chemical changes, thus, extensively alternating the properties of the polymer materials. In order to mitigate the outcome of the irradiation on the polymer films, free-radical scavengers can be introduced into the film. In this scenario, when a radical reaches the scavenger, more stable species with negligible propagation constants are formed, which further react, resulting in the formation of stable compounds. In other words, the presence of stabilizers alternates the pathway of the polymer film interaction with γ radiation, providing significant resistance toward radical-induced degradation. In our work, we explored several strategies for radical scavenging.

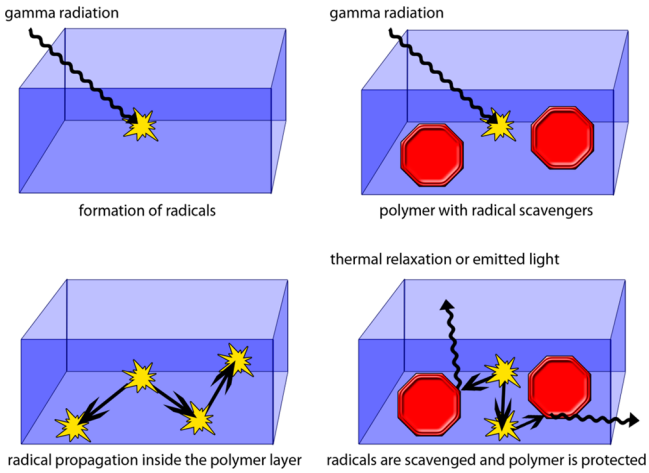

Figure 3. Scheme depicting γ radiation damage (left) of the grafted polymer layers and strategy for the damage mitigation (right), where radical scavengers protecting polymer by terminating radical propagation within the film.

Grafting of PS to PGMA Film. In order to increase the stability of the PGMA film toward ionizing radiation, it can be modified with further grafting of the macromolecules that are robust against the radiation. Polystyrene, where the presence of the aromatic rings provides effective scavenging of the radicals,

DOI: 10.1021/acsami.5b05863
ACS Appl. Mater. Interfaces 2015, 7, 19455–19465

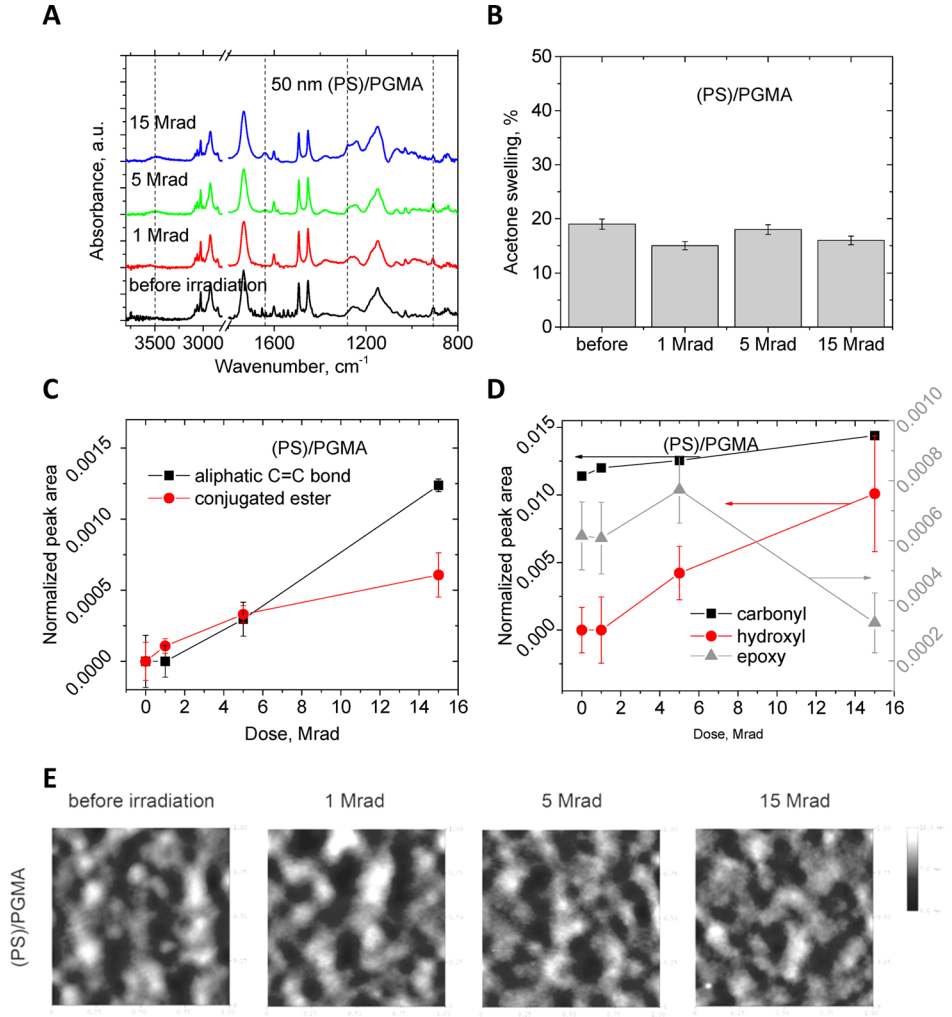

Figure 4. Gamma irradiation effects on PGMA grafted film modified with PS grafting. (a) FTIR spectra of PS/PGMA film before irradiation, after 1 and 15 Mrad gamma irradiation; (b) swelling extent in acetone vapor upon γ radiation; (c) the areas of aliphatic carbon−carbon double bond and conjugated ester normalized by PGMA content as a function of irradiation dose; (d) the areas of carbonyl, hydroxyl (left axis) and epoxy (right axis) peaks normalized by PGMA content as a function of irradiation dose; (e) AFM images (height bar is 10 nm, scan size 1 μm by 1 μm). Lines are guide for eyes only.

has high resistance toward the radiation,[56,57,62] which makes it a perfect candidate to be a stabilizer. For instance, for the poly(methyl acrylate)-PS copolymer, in situ radical monitoring demonstrated that the concentration of radiation-induced radicals drops 6 times when the copolymer composition is changed from pure poly(methyl acrylate) to PS.[63] Chain scission and radiation-induced cross-linking (which are mutually opposite processes) are the general mechanisms of PMMA and PS degradation, respectively. It was confirmed, by evaluating the radiation yield (per 100 eV absorbed), that the PS tends to be cross-linked, while the chain scission is observed to be almost 4 times less for the polymer.[56] It is apparent that the PS macromolecules can be used to improve the PGMA stability toward radiation.

In order to modify the PGMA film, monocarboxy-terminated PS was deposited by dip-coating, and then melt-grafted (~25 nm) via a reaction between the carboxylic and epoxy groups into a preannealed PGMA (~25 nm) layer. In addition to the ellipsometry measurements, the presence of aromatic double bonds (peaks at 1490 and 1450 cm^{-1}) in the FTIR spectra of the grafted film confirmed the anchoring of the PS chains (Figure 4a). AFM imaging (Figure 4e) showed that roughness of the film increased from 0.2 to 1.4 nm as a result of PS grafting (SI, Table S2).

The resulting grafted films were subjected to 1, 5, and 15 Mrad of gamma-radiation and were characterized with FTIR, AFM, and ellipsometry. It appeared that the incorporation of polystyrene into the PGMA layer attains the goal of increasing the radiation stability of the film in terms of swelling (cross-linking). For the PS/PGMA layers, the extent of swelling does not decrease, even after a 15 Mrad dose (Figure 4b). It appears that the effective scavenging of the radicals by aromatic rings in the PS-modified films prevents the macromolecules constituting the layer from intensive cross-linking.

The FTIR data also indicates the efficiency of the grafted polystyrene chains as stabilizers for the PGMA nanofilms. According to the infrared data, gamma irradiation leads to the decrease in formation of hydroxyl groups, aliphatic carbon−carbon double bonds, and the disappearance of the epoxy groups (Figure 4a, c, and d). It is necessary to point out that the hydroxyl peak areas normalized to the PGMA content are almost 2 times lower for the PS/PGMA, which indicates that free radicals can be effectively captured by aromatic rings. This conjecture is confirmed by the fact that the PS/PGMA

DOI: 10.1021/acsami.5b05863
ACS Appl. Mater. Interfaces 2015, 7, 19455−19465

nanofilm demonstrates only 2-fold oxirane ring intensity loss after 15 Mrad. As consistent with the changes in the 1640 cm^{-1} carbon−carbon double bond peak area (SI, Table S1), polystyrene suppresses the double bond formation by a factor of 4 (Figures 2c and 4c). The observed phenomenon provides additional evidence of the radiation protecting efficiency of polystyrene in a PS/PGMA system. No considerable changes in the carbonyl ester peak and carbonyl ketone peak (1710 cm^{-1}) were observed for the PS/PGMA film (SI, Figure S4, Table S1). The area of the aromatic double bonds (peaks at 1490 and 1450 cm^{-1}) stays constant within the statistical errors (SI, Table S1). Therefore, the polystyrene benzene rings are not affected by gamma irradiation to the extent detectable by FTIR.

We followed the surface morphology of the PS/PGMA films in the course of gamma irradiation. It was observed that the PS/PGMA polymer layer shows significantly higher surface roughness in comparison with the base PGMA layer; however, the film is uniform at the micron level, and no dewetting was observed. As it turns out, the surface morphology of the PS/PGMA films was not affected by gamma irradiation, even at a 15 Mrad dose (Figure 4e). We determined that AFM RMS roughness for the PS/PGMA films practically does not change in course of the irradiation and stays on the level of 1.3−1.7 nm within 1 × 1 μm area (SI, Table S2).

Grafting of Hindered Amines to PGMA Film. The addition of hindered amines, which arrest the radical driven degradation of polymers, is widely used for the UV/light stabilization of polymers.[64−66] Therefore, we employed a similar strategy to increase the ionizing radiation stability of the grafted PGMA films. The mechanism of hindered amine action is complex, and involves multiple steps of radical coupling and regeneration. Since γ radiation directly creates free-radicals, hindered amine light stabilizers (HALS) may be extremely effective in preventing damage to the polymer film. For example, polypropylene stability toward γ radiation can be significantly increased by the addition of bis(2,2,6,6-tetramethyl-4-piperidinyl) decanedioate or bis(1,2,2,6,6-pentamethyl-4-piperidinyl) decanedioate at the 0.125% level.[67] HALS are scavenging radicals via the formation of nitroxide radicals, which then react with radicals formed as a result of irradiation.[66] In this respect, we selected to employ for the PGMA grafted layer stabilization, 4-amino-TEMPO, a stable nitroxide radical possessing an amino group. This group is necessary for the covalent anchoring of the molecule to the PGMA chain via the group reaction with the epoxy groups of PGMA.

The 4-amino-TEMPO was grafted into the PGMA layer by vapor grafting. It is necessary to point out that the grafting density was rather high. Specifically, the initial thickness of the PGMA layer, measured using the ellipsometer, increased from 70 to 160 nm. Analysis of the surface morphology with AFM (image is not shown) indicated that the roughness of the polymer film increased from 0.2 to 5 nm as a result of 4-amino-TEMPO anchoring (SI, Table S2). The modification of the PGMA layer has significantly decreased the extent of the acetone swelling (Figure 5a). This effect is observed because of the 4-amino-TEMPO primary amine group, which is capable of reacting twice with the epoxy rings, increasing the level of the film cross-linking.

According to the FTIR spectroscopy data, 4-amino-TEMPO is highly efficient in terms of protecting the film from changing its chemical composition: the formation of carbon−carbon double bonds was not observed, and the formation of conjugated esters is negligible (Figure 5b and SI, Table S1).

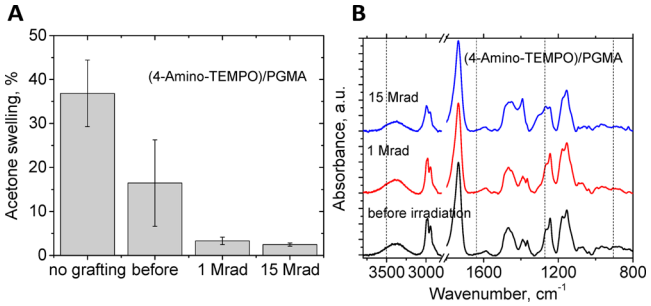

Figure 5. Gamma irradiation effects on PGMA grafted film modified with 4-amino-TEMPO. (a) Swelling extent in acetone vapor upon gamma irradiation, (b) FTIR spectra before irradiation and after 1 and 15 Mrad gamma irradiation.

We assign this type of behavior to the effective radical recombination of the free radicals formed as result of irradiation, and the stable free radicals grafted to the PGMA. The efficiency of radical scavenging is extremely high, so the chain scissions are arrested; however, the cross-linking density grows, which is reflected by the drastic decrease in swelling ability, even after 1 Mrad (Figure 5a). This important fact shows the low efficiency of the HALS and their derivatives as enrichment polymer layer stabilizers, since the excessive cross-linking leads to a decrease in the EPL's ability to interact with volatile organic compounds.

Radiation Stability of DMPS-Stabilized PGMA Films. The usage of low molecular weight compounds containing aromatic structures,[68] grafted to the main chain of the polymer being stabilized, is another approach that can lead to decreased cross-linking levels. Moreover, multiple studies show the efficiency of phenylsiloxane-based compounds as active layers or modifiers for use in sensor applications.[69−71] The high affinity of these polar polymers to the nitro compounds, coupled with relative hydrophobicity, represents significant interest in the creation of new generations of explosive detection systems. As such, phenylsiloxane/phenylsilane (e.g., DMPS) may be an effective ionizing radiation resistance additive for the polymer layer, which simultaneously increases the affinity of the polymer layer to the polar compounds.

To this end, DMPS was grafted into the PGMA nanoscale layer using the same procedure as the one used for the 4-amino-TEMPO. The initial thickness of the PGMA layer, measured by the ellipsometer, increased from 70 to 85 nm (or by 20%) during vapor grafting, via the reaction of the silanol group of DMPS with the epoxy group of PGMA. Analysis of the surface morphology with AFM (image is not shown) indicated that the roughness of the polymer film increased from 0.2 to 0.5 nm as a result of the grafting (SI, Table S2). It was found that the DMPS modification increases the extent of acetone swelling for the PGMA nanolayers (Figure 6a). First, the results indicate that there is no significant additional cross-linking of the film associated with the DMPS anchoring. We associate the swelling increase with the increased polarity in the films after grafting, due to the formation of a significant amount of hydroxyl groups, which is evident from the FTIR spectra (band located at 3500 cm^{-1}).

The grafted DMPS turned out to be an efficient ionizing radiation protection additive. In general, the additive significantly suppresses the formation of double bonds (Figure 6b and SI, Table S1), thus preventing the chemical radiation-induced changes of the chemical composition of the EPL.

DOI: 10.1021/acsami.5b05863
ACS Appl. Mater. Interfaces 2015, 7, 19455−19465

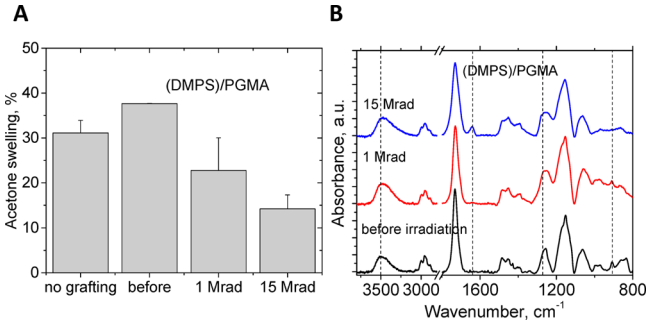

Figure 6. Gamma irradiation effects on PGMA grafted film modified by DMPS. (a) Swelling extent in acetone vapor upon γ radiation; (b) FTIR spectra before irradiation and after 1 and 15 Mrad gamma irradiation.

However, we still observed a slight increase in the bands located at 1280 and 1640 cm^{-1} as the irradiation dose increased. It was also found that the area of the carbonyl peak increases following the same trend as the nonmodified PGMA layer (SI, Table S1). The area of the hydroxyl group increases, while the epoxy peak ceases to exist after a 15 Mrad dose (SI, Table S1). The opening of the oxirane ring leads to the formation of new hydroxyl groups, in addition to the ones that have already been presented in the films after DMPS grafting.

The evaluation of the swelling in acetone was conducted in order to estimate the cross-linking suppression activity of the DMPS. It was found (Figure 6a) that irradiation significantly decreases the swelling and, therefore, increases the level of the cross-linking. In fact, the acetone swelling of the DMPS/PGMA film after 15 Mrad is almost the same as that for the nonmodified PGMA film. Therefore, the DMPS does not provide significant protection from cross-linking, while arresting the C═C bond formation.

Incorporation of Gold and BaF_2 Nanoparticles into the PGMA Film. Inorganic nanoparticles are another promising class of candidates for the protection of the polymer nanoscale layers from free-radical attacks. For instance, it is known that the addition of nanoparticles to the polymers increases their thermal stability. Zinc oxide, polyhedral oligomeric silsesquioxane (POSS), carbon nanotubes/nanoparticles, and clay particles have been intensively studied for this purpose.[72] The thermal stability increase of PMMA, modified with AlOOH, Al_2O_3, TiO_2, and Fe_2O_3 nanoparticles, is related to the following factors: the restriction of chain movements, trapping of the radicals by the surface of the nanoparticle, and chemical bonding to the metal oxide surfaces via methoxycarbonyl groups.[72] The presence of the free-radical scavenging ability encourages the use of inorganic nanoparticles for polymer film stabilization.

It is known that gold nanoparticles are capable of generating short-lived radicals by abstracting halogen or protons, with consequent scavenging of the formed radical species.[73] This effect hinders the Au nanoparticle-related organic catalysis, while providing the evidence of a strong radical affinity toward the gold surface. In order to investigate the stabilizing activity of the gold nanoparticles, hybrid organic/inorganic Au NPs/PGMA films were prepared. The concentration of the nanoparticles in the film was 16% w/w (1.3% v/v). According to the AFM imaging, the films have a smooth morphology (SI, Figure S3), and the nanoparticles are evenly distributed across the film. The RMS roughness of the Au NP containing film was on the level of 0.5 nm (SI, Table S2). In general, the particles demonstrated limited potential for polymer film protection against ionizing radiation. Specifically, the swelling of the hybrid films does not change significantly at a small radiation dose (1 Mrad) but drops considerably after 15 Mrad of gamma irradiation (Figure 7a). At the high dose, the carbon−carbon double bonds are intensively formed, as well as the hydroxyl groups (Figure 7b and SI, Table S1).

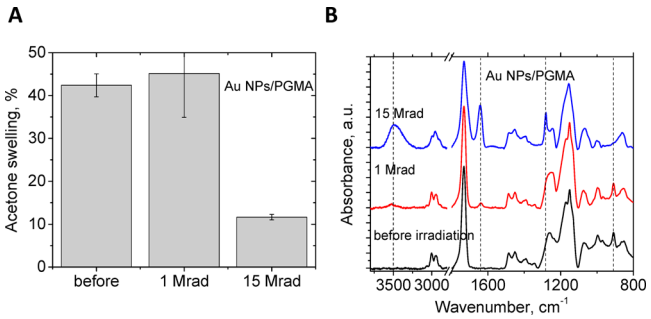

Figure 7. Gamma irradiation effects on a Au NPs/PGMA film. (a) Swelling extent in acetone vapor for the films upon gamma irradiation; (b) FTIR spectra of the film before irradiation and after 1 and 15 Mrad.

Additionally, we tested scintillator nanoparticles (BaF_2), which convert high energy ionizing radiation into light, as radiation stabilizers for the grafted nanoscale polymer layer (characteristics of the nanoparticles are provided in the SI). The PGMA/BaF_2 film contains approximately 40% w/w (12% v/v) nanoparticles, which, according to AFM imaging, are distributed within the films in small agglomerates (SI, Figure S3). The RMS roughness of the BaF_2 containing film was on the level of 4 nm (SI, Table S2). At the lower (1 Mrad) dose, these hybrid nanoscale films demonstrated a certain stability toward gamma irradiation. For the higher irradiation dose (15 Mrad), the extensive formation of the double bonds (Figure 8a

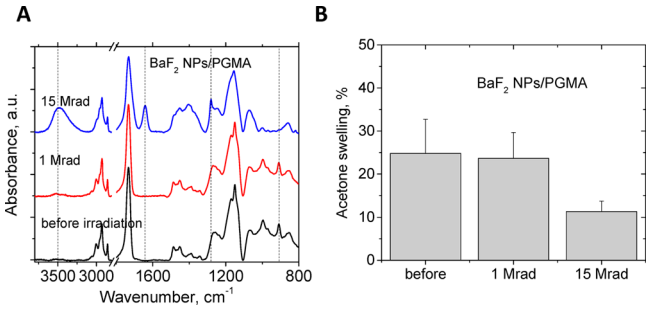

Figure 8. Gamma irradiation effects on the BaF_2 NPs/PGMA polymer layer. (a) FTIR spectra before irradiation and after 1 and 15 Mrad gamma irradiation; (b) swelling extent in acetone vapor upon γ radiation.

and SI, Table S1), as well as film cross-linking (Figure 8b), was clearly observed. An increase in the carbonyl peak area also occurs while the irradiation dose increases (SI, Table S1). Thus, the BaF_2 nanoparticles are actually protecting the film from gamma irradiation; however, this effect is weaker than that for the (macro)molecular stabilizers.

Comparison of the Radiation Stabilizer Efficiencies. According to the comparative normalized FTIR spectra (Figure 9a,b), the stability of the nanoscale film stabilizers is estimated as the area of the carbon−carbon double bond formation

DOI: 10.1021/acsami.5b05863
ACS Appl. Mater. Interfaces 2015, 7, 19455−19465

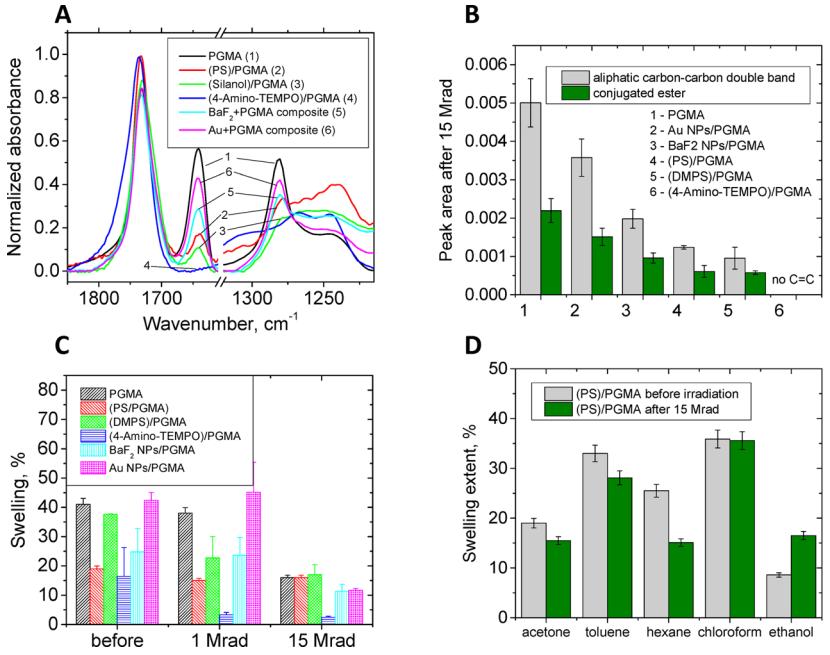

Figure 9. (a) FTIR spectra of grafted polymer films with magnified carbonyl/C═C and conjugated ester regions; (b) the intensity of double bond and conjugated ester peaks normalized by layer thickness for PGMA, Au NPs/PGMA, BaF_2 NPs/PGMA, PS/PGMA, DMPS/PGMA, and 4-amino-TEMPO/PGMA polymer films; (c) swelling of PGMA, Au NPs/PGMA, BaF_2 NPs/PGMA, PS/PGMA, DMPS/PGMA, and (4-amino-TEMPO)/PGMA enrichment polymer layers in acetone; (d) swelling of PS/PGMA films in acetone, toluene, hexane, chloroform, and ethanol before and after 15 Mrad irradiation.

changes in the following order: 4-amino-TEMPO > DMPS > PS > BaF_2 NPs > Au NPs > pure PGMA. Whereas the cross-linking suppression activity changes in a different order (Figure 9c): PS ≫ DMPS ≈ BaF_2NPs ≈ AuNPs ≈ pure PGMA ≫ 4-amino-TEMPO. Despite the fact that the DMPS and 4-amino-TEMPO provided more significant protection against the radiation-related chemical changes, PS is a more promising candidate for the sensing application, because it is not undergoing extensive cross-linking, even after the high dose (15 Mrad), and continues to show the same swelling extent as the nonirradiated film.

However, since the EPLs are intended for use in chemical detection systems, the changes in the chemical affinity of the PS/PGMA layers should be estimated, to evaluate the probability of false-positives and false-negatives in the EPL-based sensors. In order to do this, the irradiated and nonirradiated PS/PGMA films were exposed to a group of solvents with different polarities. In the experiment, we estimated that the affinity of the film toward acetone, chloroform, and toluene does not change significantly upon irradiation (Figure 9d). However, the PS/PGMA layer shows a significant increase in the polar ethanol and decrease in the nonpolar hexane swelling extent upon irradiation. These results indicate that chemical changes influence the nanoscale polymer layer response, after gamma irradiation. Specifically, we suggest that the formation of the hydroxyl groups (Figure 4d) increases the polarity of the nanoscale film, which is responsible for the observed changes in the extents of the ethanol and hexane swelling.

CONCLUSIONS

We have studied the influence of gamma irradiation on nanoscale PGMA grafted films and identified avenues for improving their stability toward ionizing radiation. In terms of applications, we concentrated on EPLs, which are polymer thin films employed in sensor devices. First of all, it was determined that for pure PGMA layers, a significant level of cross-linking was observed due to irradiation. The cross-linking is accompanied by the formation of conjugated ester, carbon double bonds, hydroxyl groups, ketone carbonyls, and the elimination of epoxy groups. PS, DMPS, 4-amino-TEMPO, BaF_2, and gold nanoparticles were incorporated into the films and were found to mitigate different aspects of the radiation damage. Finally, PS was found to be the most effective stabilizer with respect to the application of PGMA films as EPLs.

ASSOCIATED CONTENT

Supporting Information

The Supporting Information is available free of charge on the ACS Publications website at DOI: 10.1021/acsami.5b05863.

(a) Characteristics of BaF_2 nanoparticles, (b) morphology of PGMA/nanoparticles films, (c) carbonyl peak deconvolution, and (d) areas of the FTIR peaks (PDF)

AUTHOR INFORMATION

Corresponding Author

*E-mail: luzinov@clemson.edu.

Notes

The authors declare no competing financial interest.

ACKNOWLEDGMENTS

Funding for this work has been provided by the Defense Threat Reduction Agency (Projects HDTRA1-10-1-0101 and HDTRA1-13-1-0001).

DOI: 10.1021/acsami.5b05863
ACS Appl. Mater. Interfaces 2015, 7, 19455−19465

REFERENCES

(1) Huang, X.; Han, S.; Huang, W.; Liu, X. Enhancing Solar Cell Efficiency: the Search for Luminescent Materials as Spectral Converters. *Chem. Soc. Rev.* **2013**, *42*, 173−201.

(2) Cho, B.; Kim, T.-W.; Song, S.; Ji, Y.; Jo, M.; Hwang, H.; Jung, G.-Y.; Lee, T. Rewritable Switching of One Diode-One Resistor Nonvolatile Organic Memory Devices. *Adv. Mater.* **2010**, *22* (11), 1228−1232.

(3) Hu, Z. J.; Tian, M. W.; Nysten, B.; Jonas, A. M. Regular Arrays of Highly Ordered Ferroelectric Polymer Nanostructures for Non-Volatile Low-Voltage Memories. *Nat. Mater.* **2009**, *8* (1), 62−67.

(4) Ling, Q. D.; Liaw, D. J.; Zhu, C. X.; Chan, D. S. H.; Kang, E. T.; Neoh, K. G. Polymer Electronic Memories: Materials, Devices and Mechanisms. *Prog. Polym. Sci.* **2008**, *33* (10), 917−978.

(5) Wang, G.; Kim, T. W.; Lee, T. Electrical Transport Characteristics Through Molecular Layers. *J. Mater. Chem.* **2011**, *21* (45), 18117−18136.

(6) Silvi, S.; Constable, E. C.; Housecroft, C. E.; Beves, J. E.; Dunphy, E. L.; Tomasulo, M.; Raymo, F. M.; Credi, A. All-Optical Integrated Logic Operations Based on Chemical Communication between Molecular Switches. *Chem. - Eur. J.* **2009**, *15* (1), 178−185.

(7) Bundgaard, E.; Krebs, F. Low Band Gap Polymers for Organic Photovoltaics. *Sol. Energy Mater. Sol. Cells* **2007**, *91*, 954−985.

(8) Zhitenev, N. B.; Sidorenko, A.; Tennant, D. M.; Cirelli, R. A. Chemical Modification of the Electronic Conducting States in Polymer Nanodevices. *Nat. Nanotechnol.* **2007**, *2* (4), 237−242.

(9) Raymo, F. M. Digital Processing and Communication with Molecular Switches. *Adv. Mater.* **2002**, *14* (6), 401−414.

(10) Bliznyuk, V.; Galabura, Y.; Burtovyy, R.; Karagani, P.; Lavrik, N.; Luzinov, I. Electrical Conductivity of Insulating Polymer Nanoscale Layers: Environmental Effects. *Phys. Chem. Chem. Phys.* **2014**, *16* (5), 1977−1986.

(11) Chyasnavichyus, M.; Tsyalkovsky, V.; Zdyrko, B.; Luzinov, I. Tuning Fluorescent Response of Nanoscale Film With Polymer Grafting. *Macromol. Rapid Commun.* **2012**, *33* (3), 237−241.

(12) Giammarco, J.; Zdyrko, B.; Petit, L.; Musgraves, J. D.; Hu, J.; Agarwal, A.; Kimerling, L.; Richardson, K.; Luzinov, I. Towards Universal Enrichment Nanocoating for IR-ATR Waveguides. *Chem. Commun.* **2011**, *47* (32), 9104−9106.

(13) Whiting, G. L.; Snaith, H. J.; Khodabakhsh, S.; Andreasen, J. W.; Breiby, D.; Nielsen, M. M.; Greenham, N. C.; Friend, P. H.; Huck, W. T. S. Enhancement of Charge-Transport Characteristics in Polymeric Films Using Polymer Brushes. *Nano Lett.* **2006**, *6* (3), 573−578.

(14) Pinto, J. C.; Whiting, G. L.; Khodabakhsh, S.; Torre, L.; Rodriguez, A. B.; Dalgliesh, R. M.; Higgins, A. M.; Andreasen, J. W.; Nielsen, M. M.; Geoghegan, M.; Huck, W. T. S.; Sirringhaus, H. Organic Thin Film Transistors with Polymer Brush Gate Dielectrics Synthesized by Atom Transfer Radical Polymerization. *Adv. Funct. Mater.* **2008**, *18* (1), 36−43.

(15) Rutenberg, I. M.; Scherman, O. A.; Grubbs, R. H.; Jiang, W. R.; Garfunkel, E.; Bao, Z. Synthesis of Polymer Dielectric Layers for Organic Thin Film Transistors via Surface-Initiated Ring-Opening Metathesis Polymerization. *J. Am. Chem. Soc.* **2004**, *126* (13), 4062−4063.

(16) Kim, J. H.; Bohra, M.; Singh, V.; Cassidy, C.; Sowwan, M. Smart Composite Nanosheets with Adaptive Optical Properties. *ACS Appl. Mater. Interfaces* **2014**, *6* (16), 13339−13343.

(17) Chen, C. M.; Niu, X. Y.; Han, C.; Shi, Z. S.; Wang, X. B.; Sun, X. Q.; Wang, F.; Cui, Z. C.; Zhang, D. M. Reconfigurable Optical Interleaver Modules with Tunable Wavelength Transfer Matrix Function Using Polymer Photonics Lightwave Circuits. *Opt. Express* **2014**, *22* (17), 19895−19911.

(18) Akiyama, Y.; Sodaye, H.; Shibahara, Y.; Honda, Y.; Tagawa, S.; Nishijima, S. Study on Gamma-Ray-Induced Degradation of Polymer Electrolyte by pH Titration and Solution Analysis. *Polym. Degrad. Stab.* **2010**, *95* (1), 1−5.

(19) O'Donnell, J., Chemistry of Radiation Degradation of Polymers. In *Radiation Effects on Polymers*; Clough, R. L. S. S.W., Ed.; American Chemical Society: Washington, DC, 1991; pp 402−413.

(20) Fried, J. R. *Polymer Science and Technology*, 3rd ed.; Prentice Hall: Upper Saddle River, NJ, 2014; p 663.

(21) Kudoh, H.; Sasuga, T.; Seguchi, T. High Energy Ion Irradiation Effects on Polymer Materials—LET Dependence of G Value of Scission of Polymethylmethacrylate (PMMA). *Radiat. Phys. Chem.* **1997**, *50* (3), 299−302.

(22) Bhattacharya, A. Radiation and Industrial Polymers. *Prog. Polym. Sci.* **2000**, *25* (3), 371−401.

(23) Busfield, W.; O'Donnell, J. Effects of Gamma Radiation on Copolymers of Styrene and Methyl Methacrylate in the Solid State. *J. Polym. Sci., Polym. Symp.* **1975**, *49*, 227−237.

(24) Moore, J. A.; Jin, J. O. Degradation of Poly(methyl methacrylate): Deep UV, X-ray, Electron-Beam, and Proton-Beam Irradiation. In *Radiation effects on polymers*; Clough, R. L., Shalaby, S. W., Eds.; American Chemical Society: Washington, DC, 1991; pp 156−192.

(25) Bazani, D. L. M.; Lima, J. P. H.; de Andrade, A. M. MEH-PPV Thin Films for Radiation Sensor Applications. *IEEE Sens. J.* **2009**, *9* (7), 748−751.

(26) Lima Pacheco, A. P.; Araujo, E. S.; de Azevedo, W. M. Polyaniline/Poly Acid Acrylic Thin Film Composites: a New Gamma Radiation Detector. *Mater. Charact.* **2003**, *50* (2−3), 245−248.

(27) Laranjeira, J. M. G.; Khoury, H. J.; de Azevedo, W. M.; de Vasconcelos, E. A.; da Silva, E. F. Polyaniline nanofilms as a monitoring label and dosimetric device for gamma radiation. *Mater. Charact.* **2003**, *50* (2−3), 127−130.

(28) Kaoumi, D.; Weber, W. J.; Hattar, K.; Ribis, J. Introduction: Characterization and Modeling of Radiation Damage on Materials: State of the Art, Challenges, and Protocols. *J. Mater. Res.* **2015**, *30* (9), 1157−1157.

(29) Lee, J.-R.; Park, S.-J.; Seo, M.-K.; Baik, Y.-K.; Lee, S.-K. A Study on Physicochemical Properties of Epoxy Coating System for Nuclear Power Plants. *Nucl. Eng. Des.* **2006**, *236* (9), 931−937.

(30) McQuade, D. T.; Pullen, A. E.; Swager, T. M. Conjugated Polymer-Based Chemical Sensors. *Chem. Rev.* **2000**, *100*, 2537−74.

(31) Harsányi, G. Polymeric Sensing Films: New Horizons in Sensorics? *Mater. Chem. Phys.* **1996**, *43* (1−3), 199−203.

(32) Thomas, S. W.; Joly, G. D.; Swager, T. M. Chemical Sensors Based on Amplifying Fluorescent Conjugated Polymers. *Chem. Rev.* **2007**, *107*, 1339−86.

(33) Hu, X.; Fan, Y.; Zhang, Y.; Dai, G.; Cai, Q.; Cao, Y.; Guo, C. Molecularly Imprinted Polymer Coated Solid-Phase Microextraction Fiber Prepared by Surface Reversible Addition-Fragmentation Chain Transfer Polymerization for Monitoring of Sudan Dyes in Chilli Tomato Sauce and Chilli Pepper Samples. *Anal. Chim. Acta* **2012**, *731*, 40−8.

(34) Meilikhov, M.; Furukawa, S.; Hirai, K.; Fischer, R. A.; Kitagawa, S. Binary Janus Porous Coordination Polymer Coating for Sensor Devices with Tunable Analyte Affinity. *Angew. Chem., Int. Ed.* **2013**, *52* (1), 341−345.

(35) David, N. A.; Wild, P. M.; Djilali, N. Parametric Study of a Polymer-Coated Fibre-Optic Humidity Sensor. *Meas. Sci. Technol.* **2012**, *23* (3), 8.

(36) Lin, P. T.; Giammarco, J.; Borodinov, N.; Savchak, M.; Singh, V.; Kimerling, L. C.; Tan, D. T. H.; Richardson, K. A.; Luzinov, I.; Agarwal, A. Label-Free Water Sensors Using Hybrid Polymer-Dielectric Mid-Infrared Optical Waveguides. *ACS Appl. Mater. Interfaces* **2015**, *7* (21), 11189−94.

(37) Singh, V.; Lin, P. T.; Patel, N.; Lin, H.; Li, L.; Zou, Y.; Deng, F.; Ni, C.; Hu, J.; Giammarco, J.; Soliani, A. P.; Zdyrko, B.; Luzinov, I.; Novak, S.; Novak, J.; Wachtel, P.; Danto, S.; Musgraves, J. D.; Richardson, K.; Kimerling, L. C.; Agarwal, A. M. Mid-Infrared Materials and Devices on a Si Platform for Optical Sensing. *Sci. Technol. Adv. Mater.* **2014**, *15* (1), 014603.

(38) Zdyrko, B.; Klep, V.; Luzinov, I. Synthesis and Surface Morphology of High-Density Poly(ethylene glycol) Grafted Layers. *Langmuir* **2003**, *19* (24), 10179−10187.

DOI: 10.1021/acsami.5b05863
ACS Appl. Mater. Interfaces 2015, 7, 19455−19465

(39) Jacobsohn, L. G.; Sprinkle, K. B.; Roberts, S. a.; Kucera, C. J.; James, T. L.; Yukihara, E. G.; DeVol, T. A.; Ballato, J. Fluoride Nanoscintillators. *J. Nanomater.* **2011**, *2011*, 1−6.
(40) Jacobsohn, L. G.; Kucera, C. J.; James, T. L.; Sprinkle, K. B.; DiMaio, J. R.; Kokuoz, B.; Yazgan-Kukouz, B.; DeVol, T. A.; Ballato, J. Preparation and Characterization of Rare Earth Doped Fluoride Nanoparticles. *Materials* **2010**, *3* (3), 2053−2068.
(41) Tsyalkovsky, V.; Burtovyy, R.; Klep, V.; Lupitskyy, R.; Motornov, M.; Minko, S.; Luzinov, I. Fluorescent Nanoparticles Stabilized by Poly(ethylene glycol) Containing Shell for pH-Triggered Tunable Aggregation in Aqueous Environment. *Langmuir* **2010**, *26* (13), 10684−10692.
(42) Galabura, Y.; Soliani, A. P.; Giammarco, J.; Zdyrko, B.; Luzinov, I. Temperature Controlled Shape Change of Grafted Nanofoams. *Soft Matter* **2014**, *10* (15), 2567−2573.
(43) Liu, Y.; Klep, V.; Zdyrko, B.; Luzinov, I. Synthesis of High-Density Grafted Polymer Layers with Thickness and Grafting Density Gradients. *Langmuir* **2005**, *21* (25), 11806−11813.
(44) Zdyrko, B.; Luzinov, I. Polymer Brushes by the ″Grafting to″ Method. *Macromol. Rapid Commun.* **2011**, *32* (12), 859−869.
(45) Iyer, K. S.; Luzinov, I. Effect of Macromolecular Anchoring Layer Thickness and Molecular Weight on Polymer Grafting. *Macromolecules* **2004**, *37* (25), 9538−9545.
(46) Zdyrko, B.; Klep, V.; Li, X. W.; Kang, Q.; Minko, S.; Wen, X. J.; Luzinov, I. Polymer Brushes as Active Nanolayers for Tunable Bacteria Adhesion. *Mater. Sci. Eng., C* **2009**, *29* (3), 680−684.
(47) Samadi, A.; Husson, S. M.; Liu, Y.; Luzinov, I.; Kilbey, S. M. Low-Temperature Growth of Thick Polystyrene Brushes via ATRP. *Macromol. Rapid Commun.* **2005**, *26* (23), 1829−1834.
(48) Hoy, O.; Zdyrko, B.; Lupitskyy, R.; Sheparovych, R.; Aulich, D.; Wang, J. F.; Bittrich, E.; Eichhorn, K. J.; Uhlmann, P.; Hinrichs, K.; Muller, M.; Stamm, M.; Minko, S.; Luzinov, I. Synthetic Hydrophilic Materials with Tunable Strength and a Range of Hydrophobic Interactions. *Adv. Funct. Mater.* **2010**, *20* (14), 2240−2247.
(49) Peng, J. S.; Ming, L.-J.; Lin, Y.-S.; Lee, S. EPR Study of Radical Annihilation Kinetics of γ-Ray-Irradiated Acrylic (PMMA) at Elevated Temperatures. *Polymer* **2011**, *52*, 6090−6096.
(50) Sousa, A. R.; Araújo, E. S.; Carvalho, A. L.; Rabello, M. S.; White, J. R. The Stress Cracking Behaviour of Poly(methyl methacrylate) after Exposure to Gamma Radiation. *Polym. Degrad. Stab.* **2007**, *92* (8), 1465−1475.
(51) Muisener, P. A. O.; Clayton, L.; D'Angelo, J.; Harmon, J. P.; Sikder, A. K.; Kumar, A.; Cassell, A. M.; Meyyappan, M. Effects of Gamma Radiation on Poly(methyl methacrylate)/Single-Wall Nanotube Composites. *J. Mater. Res.* **2002**, *17* (10), 2507−2513.
(52) Araujo, P. L. B. Polyaniline Nanofibers as a New Gamma Radiation Stabilizer Agent for PMMA. *eXPRESS Polym. Lett.* **2007**, *1*, 385−390.
(53) Williams, J. L. Stability of polypropylene to gamma radiation. In *Radiation effects on polymers*; Clough, R. L., Shalaby, S. W., Eds.; American Chemical Society: Washington, DC, 1991; pp 554−568.
(54) Choi, J. O.; Moore, J. A.; Corelli, J. C.; Silverman, J. P.; Bakhru, H. Degradation of Poly(methylmethacrylate) by Deep Ultraviolet, X-Ray, Electron-Beam, and Proton-Beam Irradiations. *J. Vac. Sci. Technol., B: Microelectron. Process. Phenom.* **1988**, *6* (6), 2286−2289.
(55) Miller, K. J.; Hellman, J. H.; Moore, J. A. Conformations of Poly(methyl methacrylate) and its Degraded Forms Upon Radiation. *Macromolecules* **1993**, *26* (18), 4945−4952.
(56) Busfield, W.; O'Donnell, J. Effects of Gamma Radiation on Copolymers of Styrene and Methyl Methacrylate in the Solid State. *J. Polym. Sci., Polym. Symp.* **1975**, *49* (1), 227−237.
(57) Busfield, W. K.; O'Donnell, J. H.; Smith, C. A. Radiation Degradation of Poly(styrene-co-methylmethacrylate). 2. Protective Effects of Styrene on Volatile Products, Chain Scission and Flexural Strength. *Polymer* **1982**, *23* (3), 431−434.
(58) Shultz, A. R.; Roth, P. I.; Rathmann, G. B. Light Scattering and Viscosity Study of Electron-Irradiated Polystyrene and Polymethacrylates. *J. Polym. Sci.* **1956**, *22* (102), 495−507.
(59) Gedan-Smolka, M.; Lehmann, D.; Cetin, S. Basic Investigations for Development of New Curing Mechanisms for Powder Coatings. *Prog. Org. Coat.* **1998**, *33* (3−4), 177−185.
(60) Welp, K. A.; Wool, R. P.; Agrawal, G.; Satija, S. K.; Pispas, S.; Mays, J. Direct Observation of Polymer Dynamics: Mobility Comparison between Central and End Section Chain Segments. *Macromolecules* **1999**, *32*, 5127−5138.
(61) Güven, O.; Alacakir, A.; Tan, E. An Atomic Force Microscopic Study of the Surfaces of Polyethylene and Polycarbonate Films Irradiated with Gamma Rays. *Radiat. Phys. Chem.* **1997**, *50* (2), 165−170.
(62) Bowmer, T.; Cowen, L. Degradation of Polystyrene by Gamma Irradiation: Effect of Air on the Radiation Induced Changes in Mechanical and Molecular Properties. *J. Appl. Polym. Sci.* **1979**, *24* (2), 425−439.
(63) Kellman, R.; Hill, D. T. J.; Hunter, D. S.; O'Donnell, J.; Pomery, P. J. Gamma Radiolysis of Styrene-co-Methyl Acrylate Copolymers: an Electron Spin Resonance Study. In *Radiation effects on polymers*; Clough, R. L., Shalaby, S. W., Eds.; American Chemical Society: Washington, DC, 1991; pp 119−134.
(64) Gou, X.; Liu, D.; Hua, C.; Zhao, J.; Zhang, W. Synthesis and Properties of Multifunctional Hindered Amine Light Stabilizers. *Heterocycl. Commun.* **2014**, *20* (1), 15−20.
(65) Paine, M. R. L.; Barker, P. J.; Blanksby, S. J. Characterising In Situ Activation and Degradation of Hindered Amine Light Stabilisers Using Liquid Extraction Surface Analysis-Mass Spectrometry. *Anal. Chim. Acta* **2014**, *808*, 190−8.
(66) Malatesta, V.; Neri, C.; Ranghino, G. Molecular Mechanics and Dynamics Studies of Polysiloxane-Based Hindered Amine Light Stabilizers (HALS). *Macromolecules* **1993**, *26*, 4287−4292.
(67) Falicki, S.; Gosciniak, D. J.; Cooke, J. M.; Cooney, J. D.; Carlsson, D. J. Polypropylene Stabilization During Gamma Irradiation and during Post-Gamma Storage. *Polym. Degrad. Stab.* **1994**, *43* (1), 117−124.
(68) Garcia-Uriostegui, L.; Dionisio, N.; Burillo, G. Evaluation of 2-vinylnaphthalene and 4-vinylbiphenyl as Antirads to Increase the Radiation Resistance of Poly(vinyl chloride). *Polym. Degrad. Stab.* **2013**, *98* (7), 1407−1412.
(69) Mlsna, T. E.; Cemalovic, S.; Warburton, M.; Hobson, S. T.; Mlsna, D. a.; Patel, S. V. Chemicapacitive Microsensors for Chemical Warfare Agent and Toxic Industrial Chemical Detection. *Sens. Actuators, B* **2006**, *116* (1−2), 192−201.
(70) Patel, S. V.; Mlsna, T. E.; Fruhberger, B.; Klaassen, E.; Cemalovic, S.; Baselt, D. R. Chemicapacitive Microsensors for Volatile Organic Compound Detection. *Sens. Actuators, B* **2003**, *96* (3), 541−553.
(71) Dedeoglu, B.; Aviyente, V.; Ozen, A. S. Computational Insight into the Explosive Detection Mechanisms in Silafluorene- and Silole-Containing Photoluminescent Polymers. *J. Phys. Chem. C* **2014**, *118* (12), 6385−6397.
(72) Chrissafis, K.; Bikiaris, D. Can Nanoparticles Really Enhance Thermal Stability of Polymers? Part I: An Overview on Thermal Decomposition of Addition Polymers. *Thermochim. Acta* **2011**, *523*, 1−24.
(73) Ionita, P.; Spafiu, F.; Ghica, C. Dual Behavior of Gold Nanoparticles, as Generators and Scavengers for Free Radicals. *J. Mater. Sci.* **2008**, *43* (19), 6571−6574.

DOI: 10.1021/acsami.5b05863
ACS Appl. Mater. Interfaces 2015, 7, 19455−19465